resources

MDPI

Project Report

Improving the Efficiency of Pyrolysis and Increasing the Quality of Gas Production through Optimization of Prototype Systems

Csaba Fogarassy [1,*], Laszlo Toth [2], Marton Czikkely [1,*] and David Christian Finger [3]

[1] Climate Change Economics Research Centre, Faculty of Economics and Social Sciences, Szent Istvan University, 2100 Gödöllö, Hungary
[2] Faculty of Mechanical Engineering, Szent Istvan University, 2100 Gödöllö, Hungary; toth.laszlo@gek.szie.hu
[3] School of Science and Engineering, Reykjavik University, 101 Reykjavik, Iceland; davidf@ru.is
* Correspondence: fogarassy.csaba@gtk.szie.hu (C.F.); czikkely.marton@gtk.szie.hu (M.C.)

Received: 13 November 2019; Accepted: 13 December 2019; Published: 15 December 2019

Abstract: Pyrolysis is a thermochemical process that consists of the degradation of organic polymers and biomass minerals in lignocellulose materials. At low pyrolysis temperature (300–400 °C), primarily carbon is produced during the reaction time. Rapid pyrolysis takes place at temperatures between 500 and 650 °C. If the temperature is higher than 700 °C, the final product is methane, also known as biogas. The pyrolysis generator can be combined with a small power plant (CHP), which is a promising technology because the unit can be installed directly near the biomass production, and electricity can be fed de-centrally to the public utility network, while there are several possibilities for using waste heat in local systems. Carbonaceous ash can be utilized well in the agricultural field, because, in areas with intensive farming, the soil suffers from carbon and mineral deficiencies, and the phenomenon of material defect can be reduced by a proper level of implementation. This study describes the technical content of the biochar pilot project, and then, through a detailed presentation of the experimental results, we interpret the new scientific results. Our aim is to improve the quality of the produced gas by increasing the efficiency of the pyrolysis generator. In order for the pyrolysis unit to operate continuously, with proper efficiency and good gas quality, it is necessary to optimize the operation process. Our review reveals that the use of vibration may be advantageous during pyrolysis, which affects the mass of the pyrolysis carbon in a plane. Accordingly, the application of vibration to the input section of the funnel might enhance the quality of the gas, as well. The study concludes that more accurate dimensioning of the main parts of the gas reactor and a more convenient design of the oxidation and reduction zones enhance the good-quality gas output.

Keywords: fixed bed pyrolysis; oxidation-reduction zone; reduction of tar in gas; the significance of biomass particle size; carbon cycle

1. Description of the Developed System within the Project

Pyrolysis systems were designed based on the results of available technical resources and the authors' experience and suggestions. We refer to previous results about the design and measurement on several occasions in order to highlight the specific reasons for this solution [1–4]. Oxidation and reduction are important processes for gas quality [4]. Noncombustible gases in the pyrolysis space, as well as carbon dioxide and water, pass through the oxide field and on the glowing charcoal in the lower layer, which reduces them during further chemical reactions [5–12]. In the quality zone, the endothermic process takes place, removing heat from the environment. If you do not use a favorable temperature of 750 to 1000 °C, you will deteriorate the quality of the gas produced [13]. The release

of hydrocarbons occurs around 800 °C, with the secondary air entry into the fibered, and the gases are burned with a visible flame. The chemical processes and corresponding energy changes can be represented as follows:

$$C + CO_2 \rightarrow 2CO \ (-164.9 \text{ MJ/kg mol})$$

$$C + H_2O \rightarrow CO + H_2 \ (-122.6 \text{ MJ/kg mol})$$

$$CO + H_2O \rightarrow CO_2 + H_2 \ (+42 \text{ MJ/kg mol})$$

$$C + 2H_2 \rightarrow CH_4 \ (+75\text{MJ/kg mol})$$

$$CO_2 + H_2 \rightarrow CO + H_2O \ (-42.3\text{MJ/kg mol})$$

The proposed system differs in many respects from what is known in the literature, mainly because of the simplifications of top-fed and bottom-fed solutions [14–16].

2. Flowchart and Structure of the Developed System

The incoming biomass is transported from the site (yard) storage space to the preinstallation storage space, where it is dried to the desired moisture content. The hot gas interacting in the gas–air heat exchanger (presented in Figure 1 and Table 1) provides the heat needed for this. The direction of the processes is indicated by arrows. The air entering the oxidation space is also preheated by the air passing through a said heat exchanger. So, on the other side of this heat exchanger, the air is preheated, and then the water is injected into this airstream. This process is already taking place in the reactor space. The pressure in the total space of the reactor (from the gas discharge side) is smaller than the atmospheric pressure (due to connected vacuum pump), which also determines the direction of gas flow.

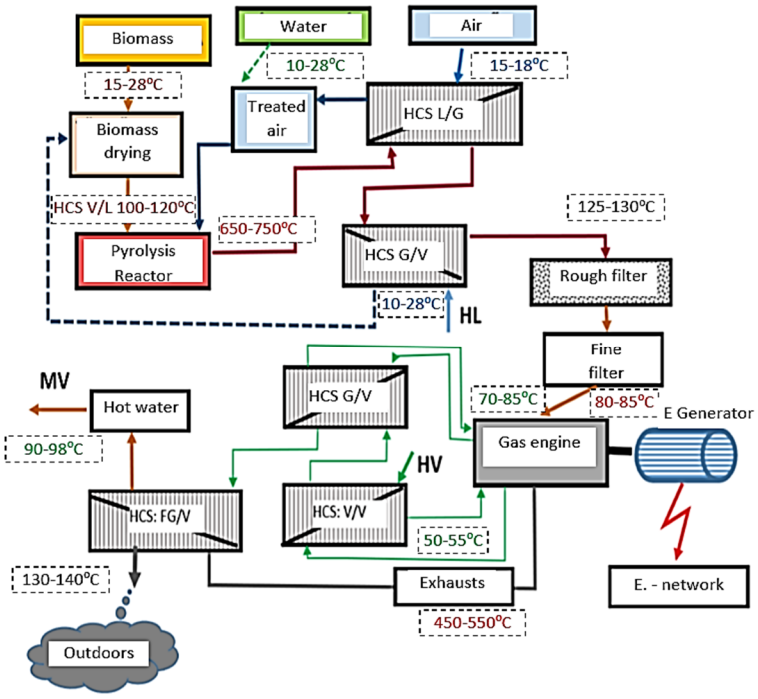

Figure 1. The flowchart of the system, with each measured temperature values (edited and designed by the authors).

The gas discharged from the lower part of the generator cools through the heat exchange, and the cooler gas enters the dust filter, where the powder is coarsely separated, and, from here, it moves on to pass through a safety filter, to get completely tar-free gas into the system [17,18]. This allows the engine to be protected from deposits in the combustion chamber. Waste heat from the engine is

presented by water/water heat exchanger. The heat exchangers serve to preheat domestic hot water. The final temperature of the domestic hot water is practically made by the high-temperature flue gas flowing out of the engine [19,20]. As a result, a clean and low-temperature flue gas is released into the environment. This is achieved by the complex system at its best efficiency. The system is illustrated in more detail in Figure 2, by marking each unit (Figure 2 and Table 2).

Table 1. The symbols and names of each part of the system (edited and designed by the authors).

Sign	Name of Each Part	Sign	Name of Each Part
HCS	Exchanger	L	Air
FG	Flue gas (Exhausts)	MV	Hot water
V	Water	HL	Cold air
G	Gas	HV	Cold water

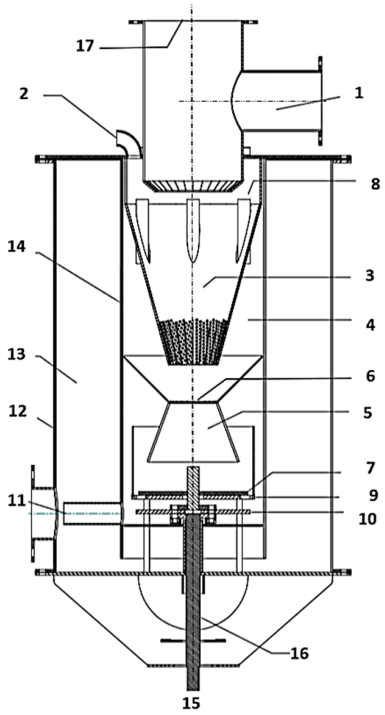

Figure 2. Schematic figure of a pyrolysis generator (edited and designed by the authors).

Items No. 3, 4, 5, and 7 were basically the subjects of the investigation, since the process of decomposition, its quality, and the performance of the equipment also depend on them. The oxidation air, as well as the recirculated gas mixture and the vapor phase, were introduced at site 2. The heated air in the heat exchanger is fed with water through a high-frequency valve, which is due to the high temperature; it is then converted into steam and fed into the oxidation/reduction zone through the nozzle No. 8.

The composition of the investigated substances, fast and slow degradation, and the effects of heating rate have already been described in detail in a previous article about this research program [21]. In the part of the equipment where the air is introduced, a certain part of the pyrolysis products is oxidized. The energy obtained here covers the heat demand of the thermal decomposition in endothermic processes. An important feature of the further zones is the decomposition of tar and its conversion into smaller molecules, which is very important for the operation of the Gary motors [22,23]. The goal was that the tar should not cross the oxidation zone. This cannot occur here at a lower temperature [24–26]. In the fixed-bed zone of the reactor model, the roasting progress takes place in the parabolic cone [27].

Table 2. Sign and names of Figure 2 (source: authors own research).

Numbers	Names of Each Part of the System
1	Fuel Feeder (Screw)
2	Preheated air, gasification aid
3	Carbonation zone (pyrolysis cone)
4	Oxidation chamber
5	Reduction zone (reduction cone)
6	Cross-section part
7	Rotating blade (scraper blade)
8	Pyrolysis gas exhaust gas pump
9	Grate
10	Rotary excavator
11	Drainage of gas
12	Gas closure outer jacket
13	Thermal insulation
14	Gas and solid baffle inner heat resistant jacket
15	Drive motor
16	Driveshaft
17	Closure cover for repair and assembly

Thus, the geometry of the oxidation zone is a fundamental and critical design factor. The thickening of the throat helps to concentrate the heat, so the airflow should be such that an equally high-temperature zone is formed throughout the cross-section (Figure 3). The complete cross-section of the incoming air (air–steam mixture) up to the wall must be filled (space 3 in Figure 3). The volume of gas flowing through the solid bed is then determined by the particle size and the upper opening of the drying space [28]. Between the upper and lower portions of the inlet portion, the inlet cross-section ratio at or near 3:2 is favorable (presented by Figures 4 and 5). The angle of the cone formed by the constriction influences the friction of the material and the downward movement thereof. The axial movement velocity of the flow of carbon and gases, i.e., the residence time in space, should be such that the maximum conversion is achieved [29,30].

In the transient double cone, the indicated narrowing is usually appropriate, but the actual dimensions depend on the particle size and size of the particles, since particle friction processes play an important role in the reduction [8,15,31–33]. It is preferred that, at the introduction of the material to be gasified, the opening between the opening and the wall is at least as wide as 10 large particles (i.e., 300–500 mm for "G50" material).

The amount of material above the pharynx increases the interaction between the surface and the particles, i.e., the friction between the sidewall and the particles. If the wall exerts a greater frictional force than the weight of the layer on a particle layer of thickness, the pressure will not increase further. The maximum pressure (in (Pa)) is calculated with Equations (1) and (2):

$$p_{max} = \frac{r\,\rho\,g}{2\mu^*} \tag{1}$$

$$P_{mv} = p_{max}\,r^2\pi = \frac{r^3\,\pi\,\rho\,g}{2\mu^*} \tag{2}$$

where r = diameter of the orifice (m), P_{mv} = downward force (N), ρ = density of the substance (kg/m^3), and μ^* = coefficient of friction between particles (varies with particle size).

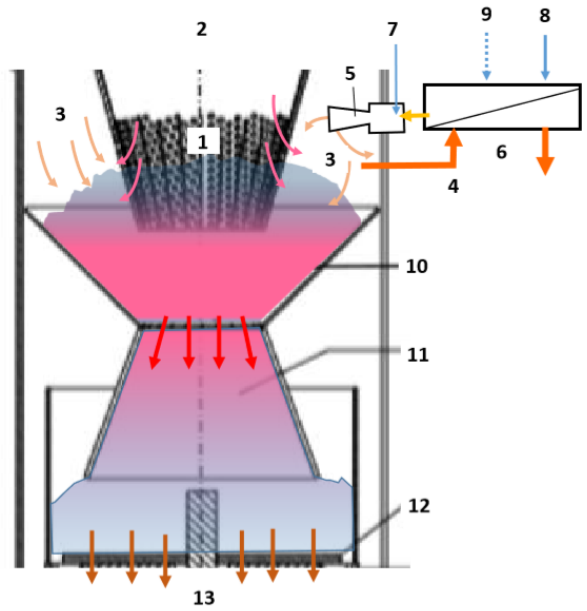

Figure 3. Functional characterization of the generator (edited and designed by the authors). Name of the numbered parts of the generator: 1—Carbonization, pyrolysis space; 2—Drying zone; 3—Oxidation chamber; 4—Primary gas; 5—Injector; 6—Exchanger; 7—Air from biomass (external pressure); 8—Heated air; 9—Water injection (from vibrating pump); 10—Double cone (reduction flow); 11—Reduction zone; 12—Rotating blade and grille; 13—Hot gas, ash, soot, carbon particles.

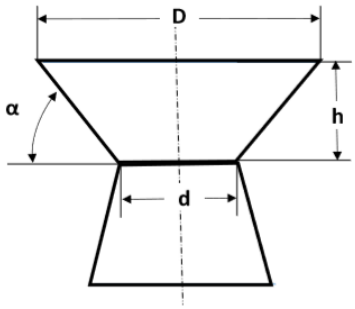

Figure 4. Double cone between oxidation and reduction zones (edited and designed by the authors).

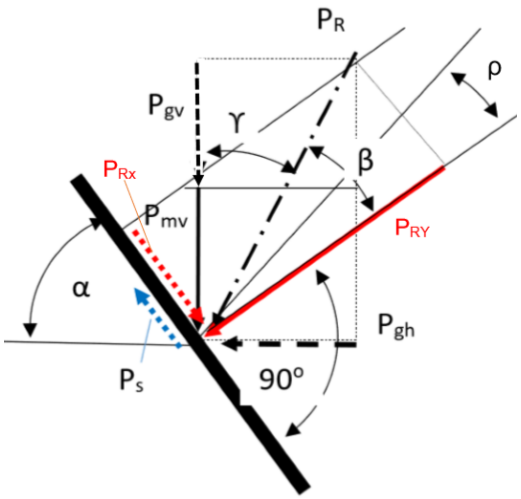

Figure 5. The cone angle and the developing force relations ($\alpha = \beta + \Upsilon$) (edited and designed by the authors).

3. The Aperture and Angle of the Reduction Cone

A practical question is whether the storage tanks are gravitationally drained or vibration is required. For example, if the radius and height of a cylindrical container are the same. When particulate material is introduced into the container, the pressure acting on the bottom of the container initially increases similarly to the hydrostatic pressure of liquids. However, the amount of material poured in increases the interaction between the sidewall and the granules, and, with it, the friction between the sidewall and the granules increases [34]. If the wall exerts a greater frictional force than the weight of the layer on a particle layer of thickness, the pressure will not increase further. Part of the weight of the cast material is supported by the sidewall, which is also subject to vertical resulting forces (presented by Figure 5). The tension in the material and the arches that block the outflow occur. The extent of this is significantly related to the quality of grinding, i.e., longer fiber residues can also be inhibitory causes [35,36]. From this point of view, the simplest experimental study of their statics is the measurement of the slope. The cast materials do not spill out; instead, they form a more or less regular cone. The angle of the cone component with the horizontal is the slope. The extent of the slope, which depends on the size, shape, and material quality of the particles, is also influenced by other operating forces besides the construction. In the present case, the gas flowing between the particles, which cause their displacement, but also the shredding knife on the lower part of the reduction basket, which also acts on the vertical force, plays a role.

The angle of the upper cone is represented by Equation (3):

$$tg\alpha = \frac{D - d}{2\,h} \tag{3}$$

where D = diameter of the oxidation zone (300 mm), d = diameter of the transition (stenosis) (100 mm), and h = height of the upper cone of the reduction zone (170 mm).

In terms of static state, a runoff occurs when the following occurs (Equation (4)):

$$P_s < P_{RX} \tag{4}$$

So, the thrust is greater than the friction (Equation (5)):

$$P_{RY}\, tg\rho < P_{RY}\, tg\beta \tag{5}$$

$$tg\rho < tg\beta$$

$$\alpha = \beta + \Upsilon$$

If α is reduced to P_S, the P_{RX} thrust will be greater, so the flow will be faster. But when α is high, the P_{RX} decreases against the frictional force (P_S), and the ability to pass is impaired. After all, the drive compression force must be greater. In an existing system, this can only be achieved by increasing the pressure difference (increasing the vacuum) [37,38].

Ultimately, P_{GV} (differential gas pressure in vacuum) = oxidation chamber pressure – vacuum at the exhaust outlet.

The friction hemispherical angle ($t_g\rho$) decreases the possibility of flow to the free outlet value in the case of a 60° inclined funnel. Above 60° for steel and carbon, ρ is already less than 8°–9°, which is less than the internal friction value, thus the tendency for arching is moderate (negligible). In practice, the resulting reaction force is overcome by the effect of differential pressure [39,40]. Flow is safe at the calculated and measured flow rate (velocity). Therefore, the cone angle was chosen to be 60°.

Model measurements with planar carbon particles (~1.0–8.0 mm) show that the runoff intensity is stable in the range of ~40°–60° (presented by Figure 6), which is advantageous for the smooth operation of the system.

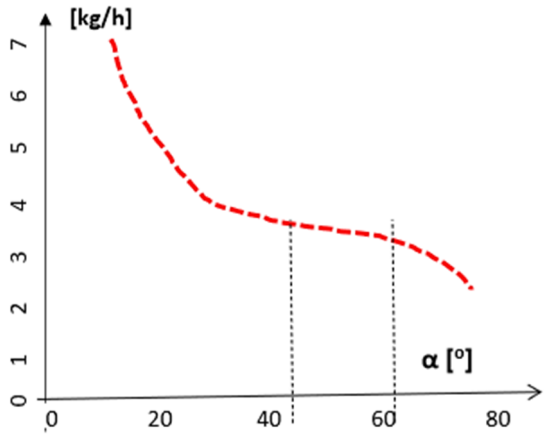

Figure 6. Mass flow as a function of α (edited and designed by the authors).

4. The Effect of Porosity

The position (porosity) of the various particles of the material, the size of the gaps (presented by Figure 7), and the "compactness" of the material determine the gas permeability of the set and thus influence the rate of reactions [41–43].

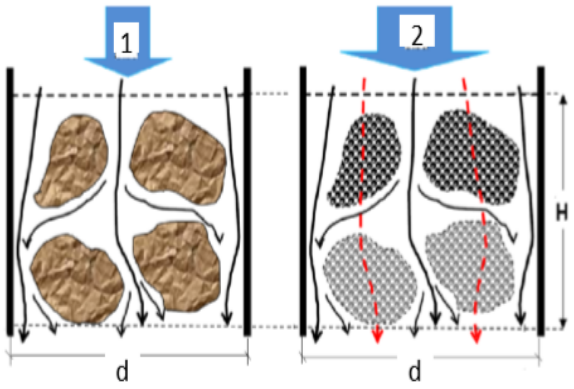

Figure 7. Typical system diagrams (1—wood granules; 2—carbon granules) (edited and designed by the authors).

Volumes and/or densities should be measured to determine porosity. The relative void volume is the value of the intergranular void volume relative to the total volume (Equation (6)):

$$\varepsilon = \frac{V_h}{V + V_h} \tag{6}$$

where V = material volume (m^3), and V_h = the so-called. gap volume (m^3).

The porosity can also be calculated from the bulk density, in which case, in addition to the volume of the particles, the volume between the particles, filled with air, must also be taken into account (Equation (7)):

$$\rho_t = \frac{m}{V + V_h} \tag{7}$$

where m = mass of the substance (kg).

The porosity with Equation (7) could be Equation (8):

$$\varepsilon = 1 - \frac{\rho_t}{\rho} \tag{8}$$

where ρ = density of original material (kg/m^3).

During pyrolysis, air or particles between the particles are removed. The product gas is flowing. The flow rate of gas through the granular medium is proportional to the pressure gradient of the system (Darcy's Law). That is the homogeneous gradient, the difference between the pressure of the gas at the upper (p_o) and lower (p_k) levels divided by the distance of the measuring points (q_g) (Equation (9)):

$$q_h = \frac{\Delta p}{h} \tag{9}$$

where $\Delta p = (p_k - p_o)$ = difference in gas pressure (P_a), and h = distance between measuring points (m).

In the discharge of gas through the grain gap, the properties of the particulate set and gas must also be taken into account (κ factor) (Equation (10)):

$$\kappa = \frac{\varepsilon\ \rho\ g}{\mu} \tag{10}$$

where ε = porosity of the particulate set, ρ = density of the gas (kg/m^3), μ = dynamic viscosity of the gas (Pa/s), and g = gravity constant (m/s^2).

The κ factor could also be called the gas conductivity of the set. Carbon from biomass is highly porous. The porosity of the inner part is generally nonuniform, typically having a small anisotropic structure, and the pores forming on the outer parts expand. The pores could be open, closed, or connected shapes. Researches show significant changes due to higher temperatures [44].

5. Effect of Adding Water and Air

The tar-reduction methods can be divided into five main groups: mechanical, system modification, thermal cracking, catalyst cracking, and plasma process. According to Phuphuakrat T. et al. [45], water and air (water vapor) have a strong influence on the tar decomposition reaction. The weight loss of gravimetric tar was 78% for thermal cracking and 77%–92% for water vapor and air intake. According to other sources, the introduction of air and H_2O in the process of pyrolysis of biomass and catalytic gasification has a significant beneficial effect [25]. During their conversion, the proportion of tar compounds is reduced during the conversion to gaseous compounds [46].

In gasification reactions above 900 °C, all effects are present [47]. The temperature of the gas produced alone should be heated to 1200 °C, to reduce the tar content to 15–20 mg/Nm^3. According to the literature, the highest cold-gas efficiency can be achieved with a carbon-dioxide-containing atmosphere. For any dosing or administration, it reduces the tar content to below the limit for engines due to gas remixing and oxidation [48].

Our aim was to improve the performance of the system, without major modifications, while keeping the gas to its permitted purity [39]. Several sources of literature have referred to this possibility. It was emphasized that the introduction of water and air into the oxidation or reduction space changes the composition of the gas and reduces the tar content. By injecting water, the water (water vapor) flowing into the open pores of the carbon particles (presented by Figure 8) dissociates into hydrogen and carbon monoxide. This also changes the composition, flammability, and energy content of the gas.

To check this, different amounts of water were injected into the system through the aforementioned injectors through the adjustability of the oscillating valves (dosing frequency). Water entering the valve was added to the pyrolysis feed air. A significant part of the water vapor/air mixture was delivered directly to the oxidation and reduction space. The results of these studies are presented in Table 3. The diagrams drawn from these illustrate the changes in the process (presented by Figures 9–11). The effect of the system temperature on the gas composition is of decisive importance, but it also influences the temperature of the reduction space when introducing the water/air mixture, but it is important to maintain the proper temperature for degradation. To achieve this, the reduction double funnel-shaped transition below the oxidation space requires the correct choice of mouth size. Proper design is important because of the residence time required for the reaction and the flow of

sufficient material. The biomass feed should match the mass flow of the glowing carbon passing through the double cone. The experiments were performed at a constant value of the output power of the equipment.

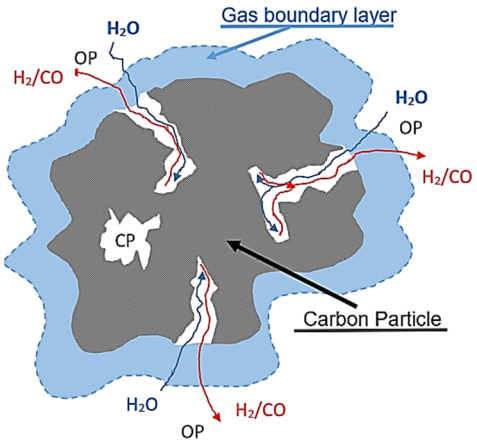

Figure 8. Conversion of water entering the pores of a high-carbon particle (edited and designed by the authors).

Table 3. Measured data after water injection (authors own research).

Performance (KW)	Air Supply (m^3/h)	Time (s)	Oxidation Temperature (°C)	Mass Flow of Water (kg/h)
5	11.25	83.2	1165	0.43
5	10.50	69.2	1150	0.52
5	10.00	55.4	1140	0.65
5	9.75	43.4	1136	0.83
5	9.25	35.6	1128	1.01
5	8.75	30.6	1116	1.18
5	8.50	26.8	1080	1.34
5	8.50	23.8	1048	1.51
5	8.50	21,2	1021	1.70
5	8.25	19.2	1010	1.88
5	8.12	17.8	1000	2.02
5	8.25	16.8	1000	2.14

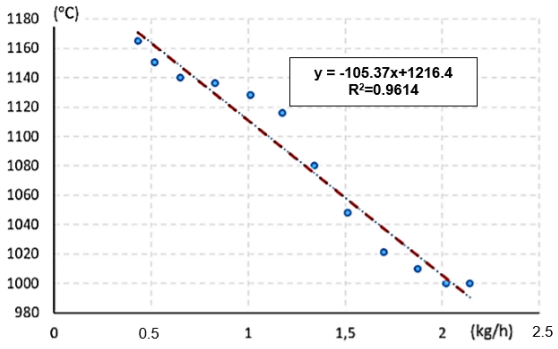

Figure 9. The effect of water intake on the temperature of the reduction space (edited and designed by the authors).

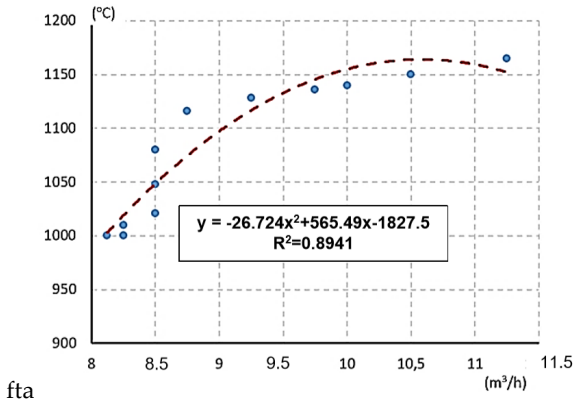

fta

Figure 10. Effect of air supply on the temperature of the reduction space (edited and designed by the authors).

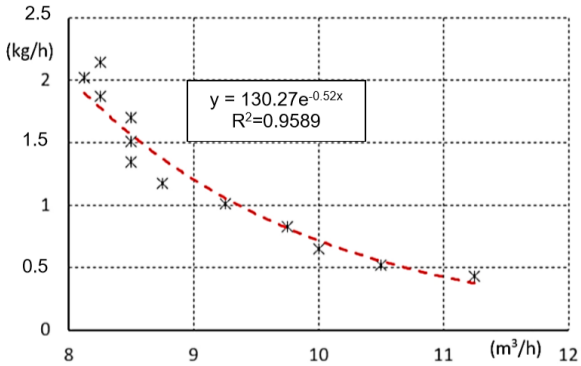

Figure 11. Relationship between air and water intake (in linear case: $y = -0.5373x + 6.1759$ and $R^2 = 0.8542$) (edited and designed by the authors).

As a result of the amount of water introduced into the vibrating valve (indicated by the frequency of vibration), the temperature of the reduction space decreased (Figure 9). From the results, it can be seen that it is not advisable to add more than 1.5 kg/h of water to the present apparatus, so that the temperature in the reduction space does not fall below 950–1000 °C. The introduction of air also has an effect on the temperature of the reduction space [49]. Given that more oxygen is introduced into the air, the combustion improves its temperature-increasing effect. The introduction of more than 9.0 to 9.5 m^3/h air volume for the reported equipment is not justified, as it would already reduce the temperature of the reduction space. It follows from the two relationships that the relationship between water and air dosing is exponentially decreasing (almost linear). It follows that, when increasing air, the amount of water should be reduced.

However, the introduction of water increases the amount of hydrogen in the gas, which is very favorable for the energy content of the gas. The amount of water intake should be used with caution since larger amounts of water reduce the temperature of the reduction space, which results in a reduction in tar degradation. In contrast, because of the air supply, the temperature of the reduction pond increases, so the optimum should be sought for the two values.

The favorable values for this unit are ~9.5 m^3/h airflow and ~1.1 kg/h water flow. This is also illustrated in Figure 11.

The literature also points out that the effect of water and air intake, as well as the remixing of the primary gas, results in a change in the composition of the gas that can be used, possibly increasing its energy content. Our experiments with the prototype equipment showed that the changes in the gas composition of this medium-sized hardwood biomass chip were significant. Because the throat diameter of the reduction cone determines the mass flow rate of the "material" to be transmitted,

the flow rate could only be adjusted to the feed materials by vibrating the mass of material in and below the cone, to aid flow. The composition of the gas, according to the final gas components, was measured with a VISIT 03H gas analyzer (Table 4).

Table 4. Water (H_2O), air (Ai), and air and gas (RG + Ai) effect of recirculation on gas composition (authors own research).

Gas Components	H_2O (%)	Ai (%)	RG + Ai (%)
C_xH_y *	1.91	1.37	1.89
H_2O	2.00	12.10	15.20
H_2	39.80	29.44	24.50
CH_4	8.47	6.01	7.44
CO	22.00	37.98	43.20
CO_2	25.83	13.10	7.76

Note: * 0.1%–0.3% of this is tar (~15–35 mg/m^3).

Due to the high temperature of the oxidation and reduction zone, the other hydrocarbon content is less than 2%. It has a tar content of 0.1%–0.3% based on the gas recovered, 15–35 mg/m^3, which does not affect the operation of the gas engines. For the production of 1.0 Nm^3 gas, 1.42–1.48 kg of air-dried hardwood (biomass) was needed.

6. Conclusions

Tests on prototype equipment have shown that fixed bed equipment produces quality biogas that is suitable for gas engines to produce fuel and CHP heat and electricity. The quality of the pyrolysis gas is fundamentally influenced by the design of the equipment, in particular, the size and shape of the reduction and oxidation spaces, and the introduction of various additives into these spaces. In order to obtain a good product, the temperature in these spaces should not change significantly. It is harmful to engine operation if the gas contains tar. When temperatures drop, the tar is not completely decomposed. Furthermore, the addition of water/air mixture changes the composition of the gas. The water supply increases the hydrogen content, but recirculation of some of the primary gas increases the CO content, and, as a result, the gas purifies less CO_2 emissions. In order for the unit to operate continuously, with sufficient efficiency, and to maintain a good gas quality, the carbonated material must be moved in the reduction space. The application of vibration to the entire system is advantageous, as it reduces the space by the use of a suitable scraper for the ash design, which exerts a planar effect on the carbon mass above it. The drive shaft of this scraper must be extended to the throat of the transitional space, the funnel.

The test prototype device may be suitable for serial production, taking into account the measured parameters. Our main goal was to improve system performance without major changes, while maintaining or increasing the purity of the gas produced. In the literature, we have found technology variants that work toward improving the purity of the gas. Introducing water and air into the oxidation or reduction space generally improves the composition of the gas and reduces the tar content. By injecting water, water (vapor) flowing into the open pores of the carbon particles dissociates into hydrogen and carbon monoxide. This changes the composition, flammability, and energy content of the gas. Measurements show that the relationship between water and air supply reduced exponentially (almost linear). It follows that, when the air is increasing, the amount of water must be reduced. In the literature, it has been pointed out that the effect of water and air intake and the remixing of the primary gas changes the composition of the usable gas and increases its energy content. Our experiments with the prototype equipment showed that the changes in the gas composition of these medium-sized hardwood biomass shavings were significant. The new result, that the mass flow of the "material" to be conveyed is determined by the throat diameter of the reducing cone, and the flow rate on the base materials can only be adjusted by vibrating the mass of the material in and below the cone, to facilitate flow.

Author Contributions: L.T. and C.F. had the initial idea for the manuscript; C.F., D.C.F, and M.C. designed the manuscript; C.F. and M.C. researched the literature; C.F. and L.T. developed the methods and integrated the literature; L.T. and C.F. wrote the manuscript; M.C. and D.C.F. supervised the project. All authors provided critical feedback and helped shape the result.

Funding: This research was funded by the Hungarian Ministry of National Economy, grant number GINOP 2.1.7-152016-01604. The Climate Change Research Centre and Doctoral School of Management and Business Administration at Szent Istvan University supported the preparation of the manuscript.

Acknowledgments: We thank the National Agricultural Research and Innovation Center Institute of Agricultural Engineering for the experimental site and the use of technical equipment. Special thanks to István Bácskai for his help in the measurements.

Conflicts of Interest: The authors declare no conflict of interest.

References

1. Saravanakumar, A.; Haridasan, T.M.; Reed, T.B.; Bai, R.K. Experimental investigation and modelling study of long stick wood gasification in a top lit updraft fixed bed gasifier. *Fuel* **2007**, *86*, 2846–2856. [CrossRef]
2. Siedlecki, M.; de Jong, W. Biomass gasification as the first hot step in clean syngas production process—Gas quality optimization and primary tar reduction measures in a 100 kW thermal input steam–oxygen blown CFB gasifier. *Biomass Bioenergy* **2011**, *35*, S40–S62. [CrossRef]
3. Thanapal, S.S.; Annamalai, K.; Sweeten, J.M.; Gordillo, G. Fixed bed gasification of dairy biomass with enriched air mixture. *Appl. Energy* **2012**, *97*, 525–531. [CrossRef]
4. Bird, R.C.; Park, S.K. The Domains of Corporate Counsel in an Era of Compliance. *Am. Bus. Law J.* **2016**, *53*, 203–249. [CrossRef]
5. Morf, P.; Hasler, P.; Nussbaumer, T. Mechanisms and kinetics of homogeneous secondary reactions of tar from continuous pyrolysis of wood chips. *Fuel* **2002**, *81*, 843–853. [CrossRef]
6. Bhattacharya, S.; Mizanur Rahman Siddique, A.H.M.; Pham, H.-L. A study on wood gasification for low-tar gas production. *Energy* **1999**, *24*, 285–296. [CrossRef]
7. Dhaundiyal, A.; Gupta, V.K. The Analysis of Pine Needles as a Substrate for Gasification. *Hydro Nepal J. Water Energy Environ.* **2014**, *15*, 73–81. [CrossRef]
8. Kihedu, J. Torrefaction and Combustion of Ligno-Cellulosic Biomass. *Energy Procedia* **2015**, *75*, 162–167. [CrossRef]
9. Patwardhan, P.R.; Brown, R.C.; Shanks, B.H. Product Distribution from the Fast Pyrolysis of Hemicellulose. *ChemSusChem* **2011**, *4*, 636–643. [CrossRef]
10. Fogarassy, C. Rationalisation of production structure of arable land energy-crops in Hungary. *Bodenkultur* **2001**, *52*, 225–231.
11. Callegari, A.; Capodaglio, A.G. Properties and Beneficial Uses of (Bio)Chars, with Special Attention to Products from Sewage Sludge Pyrolysis. *Resources* **2018**, *7*, 20. [CrossRef]
12. Ukanwa, K.S.; Patchigolla, K.; Sakrabani, R.; Anthony, E.; Mandavgane, S. A Review of Chemicals to Produce Activated Carbon from Agricultural Waste Biomass. *Sustainability* **2019**, *11*, 6204. [CrossRef]
13. Guo, F.; Dong, Y.; Dong, L.; Guo, C. Effect of design and operating parameters on the gasification process of biomass in a downdraft fixed bed: An experimental study. *Int. J. Hydrog. Energy* **2014**, *39*, 5625–5633. [CrossRef]
14. Basu, P. *Biomass Gasification and Pyrolysis: Practical Design and Theory*; Academic Press: Burlington, MA, USA, 2010; ISBN 978-0-12-374988-8.
15. Barman, N.S.; Ghosh, S.; De, S. Gasification of biomass in a fixed bed downdraft gasifier—A realistic model including tar. *Bioresour. Technol.* **2012**, *107*, 505–511. [CrossRef]
16. Raman, P.; Ram, N.K.; Gupta, R. A dual fired downdraft gasifier system to produce cleaner gas for power generation: Design, development and performance analysis. *Energy* **2013**, *54*, 302–314. [CrossRef]
17. Mondal, P.; Ghosh, S. Bio-gasification based Externally Fired Combined Cogeneration Plant: Thermo-economic Performance Analysis. In *Materials Today: Proceedings (Vol. 5, pp. 22963–22978)*; Elsevier Ltd; Available online: https://doi.org/10.1016/j.matpr.2018.11.024 (accessed on 15 December 2019).
18. Oldal, I.; Keppler, I.; Bablena, A.; Safranyik, F.; Varga, A. On the Discrete Element Modeling of Agricultural Granular Materials. *Mech. Eng. Lett. Res. Dev.* **2017**, *11*, 8–17.

19. Márta, B.; Szent István Egyetem (Gödöllő); Mezőgazdaság-és Környezettudományi Kar. *Környezetkímélő és Energiatakarékos Talajművelés*; Szent István Egyetem: Gödöllő, Hungary, 2002; ISBN 978-963-9256-80-4.
20. Ghosh, D.; Dasgupta, D.; Agrawal, D.; Kaul, S.; Adhikari, D.K.; Kurmi, A.K.; Arya, P.K.; Bangwal, D.; Negi, M.S. Fuels and Chemicals from Lignocellulosic Biomass: An Integrated Biorefinery Approach. *Energy Fuels* **2015**, *29*, 3149–3157. [CrossRef]
21. Bacskai, I.; Madar, V.; Fogarassy, C.; Toth, L. Modeling of Some Operating Parameters Required for the Development of Fixed Bed Small Scale Pyrolysis Plant. *Resources* **2019**, *8*, 79. [CrossRef]
22. Mendiburu, A.Z.; Carvalho, J.A.; Coronado, C.J.R. Thermochemical equilibrium modeling of biomass downdraft gasifier: Stoichiometric models. *Energy* **2014**, *66*, 189–201. [CrossRef]
23. Chan, W.-C.R.; Kelbon, M.; Krieger, B.B. Modelling and experimental verification of physical and chemical processes during pyrolysis of a large biomass particle. *Fuel* **1985**, *64*, 1505–1513. [CrossRef]
24. Di Blasi, C. Modeling wood gasification in a countercurrent fixed-bed reactor. *AIChE J.* **2004**, *50*, 2306–2319. [CrossRef]
25. Cao, Y.; Wang, Y.; Riley, J.T.; Pan, W.-P. A novel biomass air gasification process for producing tar-free higher heating value fuel gas. *Fuel Process. Technol.* **2006**, *87*, 343–353. [CrossRef]
26. Antonopoulos, I.-S.; Karagiannidis, A.; Elefsiniotis, L.; Perkoulidis, G.; Gkouletsos, A. Development of an innovative 3-stage steady-bed gasifier for municipal solid waste and biomass. *Fuel Process. Technol.* **2011**, *92*, 2389–2396. [CrossRef]
27. Madár, V.; Bácskai, I.; Dhaundiyal, A.; Tóth, L. Development of biomass-based pyrolisis CHP (R + D). *Hung. Agric. Eng.* **2018**, 17–23. [CrossRef]
28. Sharma, S.; Sheth, P.N. Air–Steam biomass gasification: Experiments, modeling and simulation. *Energy Convers. Manag.* **2016**, *110*, 307–318. [CrossRef]
29. Madár, V.; Tóth, L. Fagázgenerátor üzemű bio-kiserőmű és öntözőberendezés (Biogas generator and irrigation plant powered by wood gas). *Mezőgazdasági Technika* **2012**, *52*, 3–8.
30. Madár, V.; Tóth, L.; Madár, G.; Schremof, N. Kísérleti fagázgenerátor (Experimental wood gas generator). *Mezőgazdasági Technika* **2014**, *55*, 2–5.
31. Kung, H.-C. A mathematical model of wood pyrolysis. *Combust. Flame* **1972**, *18*, 185–195. [CrossRef]
32. Oldal, I. Szemcsés anyagok kifolyási és boltozódási tulajdonságai (Outflowing and arching properties of granular materials). Ph.D. Dissertation, Szent Istvan University, Gödöllő, Hungary, 2007. Available online: https://szie.hu/file/tti/archivum/Oldal_Istvan_tezis.pdf (accessed on 14 December 2019).
33. Hadroug, S.; Jellali, S.; Leahy, J.J.; Kwapinska, M.; Jeguirim, M.; Hamdi, H.; Kwapinski, W. Pyrolysis Process as a Sustainable Management Option of Poultry Manure: Characterization of the Derived Biochars and Assessment of their Nutrient Release Capacities. *Water* **2019**, *11*, 2271. [CrossRef]
34. Lászlo, T.; Csaba, F. *"Low-Carbon" Energiaellátási Rendszerek a Gyakorlatban: A Megújulóenergia-Termelés Technológiái Magyarországon (Low-Carbon Energy Supply in Practice: The Renewable Energy Production Technologies in HUNGARY)*; Szaktudás K. Ház: Gödöllő, Hungary, 2012; ISBN 978-615-5224-37-9.
35. Korzenszky, P.; Lányi, K.; Simándi, P. Test results of a pyrolysis pilot plant in Hungary. *Hung. Agric. Eng.* **2015**, 48–52. [CrossRef]
36. Borocz, M.; Herczeg, B.; Horvath, B.; Fogarassy, C. Evaluation of biochar lifecycle processes and related lifecycle assessments. *Hung. Agric. Eng.* **2016**, 60–64. [CrossRef]
37. Dhaundiyal, A.; Tewari, P. Kinetic Parameters for the Thermal Decomposition of Forest Waste Using Distributed Activation Energy Model (DAEM). *Environ. Clim. Technol.* **2017**, *19*, 15–32. [CrossRef]
38. Dhaundiyal, A.; Tewari, P.C. Performance Evaluation of Throatless Gasifier Using Pine Needles as a Feedstock for Power Generation. *Acta Technol. Agric.* **2016**, *19*, 10–18. [CrossRef]
39. Centre for Research & Technology Hellas. *15th European Biomass Conference: From Research to Market Deployment: Proceedings of the International Conference Held in Berlin, Germany, 7–11 May 2007*; European Biomass Conference, Ed.; ETA-Renewable Energies: Florence, Italy, 2007; ISBN 978-3-936338-21-8.
40. Martínez, J.D.; Silva Lora, E.E.; Andrade, R.V.; Jaén, R.L. Experimental study on biomass gasification in a double air stage downdraft reactor. *Biomass Bioenergy* **2011**, *35*, 3465–3480. [CrossRef]
41. Chen, W.-H.; Lu, K.-M.; Liu, S.-H.; Tsai, C.-M.; Lee, W.-J.; Lin, T.-C. Biomass torrefaction characteristics in inert and oxidative atmospheres at various superficial velocities. *Bioresour. Technol.* **2013**, *146*, 152–160. [CrossRef]

42. Phanphanich, M.; Mani, S. Impact of torrefaction on the grindability and fuel characteristics of forest biomass. *Bioresour. Technol.* **2011**, *102*, 1246–1253. [CrossRef]
43. Charisteidis, I.; Lazaridis, P.; Fotopoulos, A.; Pachatouridou, E.; Matsakas, L.; Rova, U.; Christakopoulos, P.; Triantafyllidis, K. Catalytic Fast Pyrolysis of Lignin Isolated by Hybrid Organosolv—Steam Explosion Pretreatment of Hardwood and Softwood Biomass for the Production of Phenolics and Aromatics. *Catalysts* **2019**, *9*, 935. [CrossRef]
44. Francioso, O.; Sanchez-Cortes, S.; Bonora, S.; Roldán, M.L.; Certini, G. Structural characterization of charcoal size-fractions from a burnt Pinus pinea forest by FT-IR, Raman and surface-enhanced Raman spectroscopies. *J. Mol. Struct.* **2011**, *994*, 155–162. [CrossRef]
45. Phuphuakrat, T.; Namioka, T.; Yoshikawa, K. Tar removal from biomass pyrolysis gas in two-step function of decomposition and adsorption. *Appl. Energy* **2010**, *87*, 2203–2211. [CrossRef]
46. Lettner, F.; Haselbacher, P.; Timmerer, H.L.; Leitner, P.; Suyitno, S.; Rasch, B. Lastest Results of CLEANSTGAS-Staged Biomass Gasification CHP. In Proceedings of the 15th European Biomass Conference and Exhibition for Research to Market Deployment, Berlin, Germany, 7–11 May 2007; pp. 1–5.
47. Wiinikka, H.; Wennebro, J.; Gullberg, M.; Pettersson, E.; Weiland, F. Pure oxygen fixed-bed gasification of wood under high temperature (\textgreater1000 °C) freeboard conditions. *Appl. Energy* **2017**, *191*, 153–162. [CrossRef]
48. Brandt, P.; Larsen, E.; Henriksen, U. High Tar Reduction in a Two-Stage Gasifier. *Energy Fuels* **2000**, *14*, 816–819. [CrossRef]
49. González, J.F.; Román, S.; Bragado, D.; Calderón, M. Investigation on the reactions influencing biomass air and air/steam gasification for hydrogen production. *Fuel Process. Technol.* **2008**, *89*, 764–772. [CrossRef]